



# Development of waterborne polyurethane dispersions (WPUDs) from novel cardanol-based reactive dispersing agent

Siddhesh U. Mestry<sup>1</sup> · Sonam P. Khuntia<sup>1</sup> · S. T. Mhaske<sup>1</sup>

Received: 20 June 2020 / Revised: 27 September 2020 / Accepted: 1 November 2020 /

Published online: 10 November 2020

© Springer-Verlag GmbH Germany, part of Springer Nature 2020, corrected publication 2020

## Abstract

The objective of the current research work is to prepare a difunctional reactive dispersing agent derived from cardanol which can be used as an alternative for dimethylol propionic acid (DMPA) in waterborne polyurethane dispersion synthesis. The novelty of the research lies between the use of bio-based resource and utilizing the sulfonic acid group as an anionic dispersible group. The cardanol was sulfonated using oleum followed by the reaction of the hydroxyl group of phenol with the epichlorohydrin (ECH). The obtained product was then hydrolyzed to generate double functionalities which can be introduced in the PU backbone through a chemical reaction with a diisocyanate. The obtained intermediates and product were characterized using hydroxyl values, epoxy equivalent weights (EEW), CHNS analysis, FTIR and <sup>1</sup>H-NMR analysis. The typical acetone process was used for the preparation of WPUDs, and the cured films were further analyzed for the various coating properties in which thermal properties showed significant improvements with the incorporation of HESC to the PU system along with the increased char yield and glass transition temperature (T<sub>g</sub>), whereas the mechanical properties did not show any improvements, which could be attributed to the bulky structure of HESC and increased rigidity in the polymeric network. The detailed synthesis, characterizations and obtained results are presented and discussed here.

**Electronic supplementary material** The online version of this article (<https://doi.org/10.1007/s00289-020-03450-7>) contains supplementary material, which is available to authorized users.

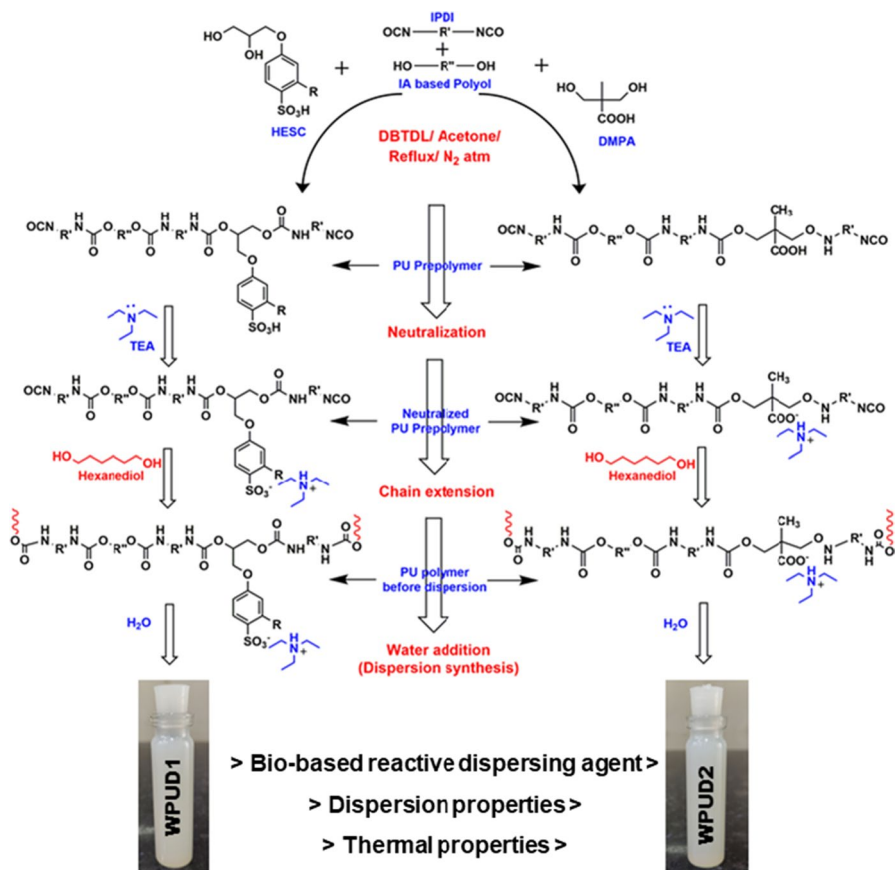
✉ S. T. Mhaske  
stmhaske@gmail.com

Siddhesh U. Mestry  
siddhesh17mestry@gmail.com

Sonam P. Khuntia  
sonampratikkhuntia@gmail.com

<sup>1</sup> Department of Polymer and Surface Engineering, Institute of Chemical Technology, Mumbai, India

## Graphic abstract



**Keywords** Sulfonation · Cardanol · Bio-based · Dispersion · Polyurethane

## Introduction

Polyurethanes (PUs) are one of the versatile materials which have the budding potential for their use in different applications like coatings [1], adhesives [2], sealants [3], elastomers, foams [4], etc. PUs offer excellent and versatile mechanical, chemical and physical properties, excellent drying ability and low-temperature flexibility which could be adjusted by adequate use of soft and hard segments. The soft segments are generally produced from polyester or polyether polyols depending upon the end application, while diisocyanates represent hard segments [5, 6]. The diisocyanates and chain extenders are immobile and stiff materials, while, on the other hand, soft segments which are can move freely which often appear in foil form.

Waterborne polyurethane dispersion (WPUD) is a binary colloidal system in which the polyurethane particles are dispersed in water as a continuous medium. The important reason for getting preferred over other forms of PU in coating systems is the reduction of solvent emission into the atmosphere, but perhaps most importantly the quality of the WPUDs has made themselves highly suitable for a wide range of applications. The hydrophilicity in WPUD is universally achieved by the use of reactive dispersing agents which can be incorporated into the polymer backbone and have the ability to drag the whole molecule into the water during the dispersion process [7]. WPUDs are classified in cationic and anionic polyurethane dispersion based on the charge on the dispersing moiety; dimethylol propionic acid (DMPA) and dimethylolbutanoic acid (DMBA) are the widely used and industrially important anionic reactive dispersing agents [8].

The anionic dispersing moieties used in WPUD synthesis can have carboxylic acid groups ( $-\text{COOH}$ ) or sulfonic acid groups ( $-\text{SO}_3\text{H}$ ). These acidic groups can be introduced in the PU backbone through the incorporation of hydrophilic polyols or chain extenders or through the reactive moieties such as DMPA as mentioned earlier. One of the inventions reported by Gabriele and co-workers [9] uses the diamine sulfonate salts having one or more sulfonic acid groups which were used as a chain extender, while another patent from Youlo et. al [10] uses the sulfonated polyester polyol as a reactive dispersant moiety. Wei and Yu [11] used dimethyl 5-sulfoisophthalate as a reactant for the preparation of sulfonated polyether polyol which was then used as an ionizable moiety in the preparation of WPUDs. Furthermore, Yang and co-workers [12] reported solvent-free sulfonated waterborne polyurethane as an advanced leather finishing material, while Feng et. al [13] report the synthesis of sulfonated graphene/WPU composites having excellent mechanical properties and wear resistance. All the aforementioned studies report the utilization of either sulfonated polyols or sulfonated chain extenders; but the very few studies report the utilization of sulfonated dispersant like 2-dihydroxypropylsulfonate, 2-hydroxyethanesulfonic acid (isethionic acid), etc. [14, 15]. Hence, owing to the fact of having varieties of applications of WPUDs and less availability of dispersants similar to DMPA in the sulfonated class, the current study targets a development of reactive dispersant having a sulfonic acid group.

Furthermore, most of the types of polyurethane systems contain a large percentage of volatile organic compounds (VOCs) which mostly turn out to be toxic and hazardous to the living organisms. Further, the raw materials which we use for the synthesis of coating systems have mostly come from the petroleum sources which are becoming the limited reservoirs. Hence, the depleting fossil fuels and stringent environmental norms drive researchers toward the development of water-based coating systems and utilization of the bio-resources [16–18]. Although the thermal properties are low in the case of polymers derived from bio-resource, the flexural strength, tensile strength, rigidity and flexibility of the WPUDs synthesized are significantly compared with the WPUDs derived from synthetic resources [19]. Cardanol is one of the bio-based reddish-brown phenolic compounds extracted from cashew nut shell liquid (CNSL) obtained from cashew fruits of the cashew tree (*Anacardium occidentale*) [20, 21]. The chemical structure of the cardanol is shown in Fig. 1. Cardanol has been extensively used in the development of plasticizers,

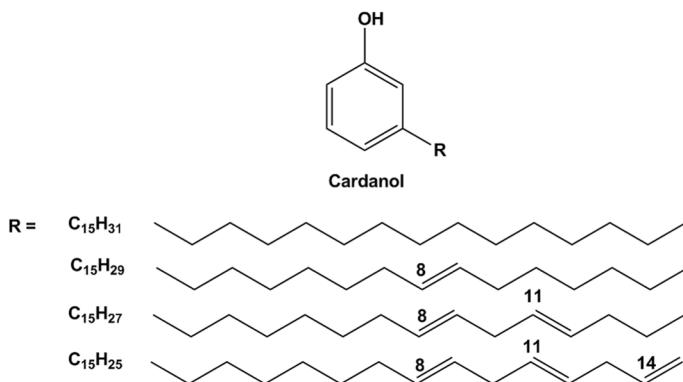


**Fig. 1** Structure of cardanol

stabilizers and laminates and for insulation purposes [22–24]. Several coatings such as epoxy, polyurethane, and waterborne coatings are derived from CNSL which demonstrates its high reactivity, adaptability to various chemistries and suitability for various applications. Various electrophilic substitution reactions can be carried out on the cardanol like other phenolic compounds which include sulfonation, nitration, Friedel–Crafts alkylation and acylation, halogenations, etc. [25–27].

The current study demonstrates, for the first time, the use of cardanol-derived reactive dispersing agent (HESC) in WPUD synthesis. The study also compares the properties of the synthesized WPUD with WPUD obtained from industrially followed dispersing agent, i.e., DMPA. The synthesis of HESC consists of sulfonation of cardanol followed by epoxidation and hydrolysis reactions. The structure of the obtained product was confirmed using Fourier transform infrared spectroscopy (FTIR), nuclear magnetic resonance (NMR) spectroscopy, hydroxyl value and CHNS analysis. HESC and DMPA were used in the synthesis of two different WPUDs keeping the same molar ratios. The obtained dispersions were characterized by particle size and zeta potential analysis for deriving the stability of the dispersion, while the obtained films were subjected to various thermal, mechanical and physical tests, and the obtained results are presented here.

## Materials and methods

### Materials

Cardanol (molecular weight=303 g/mol) was procured from Cardolite Corporation. Epichlorohydrin (ECH), triethylamine (TEA), hydrochloric acid (HCl), sodium hydroxide (NaOH), calcium oxide (CaO), acetone, ethyl acetate (EA), toluene, anhydrous sodium sulfate ( $Na_2SO_4$ ), itaconic acid, tetrabutylammoniumbromide (TBAB) and 1,6- hexanediol (HD) were purchased from S D Fine Chemicals Limited, India. Dibutyltin dilaurate (DBTDL), 1,6-hexanediol, oleum (20%) were obtained from

Sigma-Aldrich, India, while isophorone diisocyanate (IDPI) was obtained from Alfa Aesar, India. All the chemicals were used as received without any treatment. The mild steel panels were used as the substrates for the coating application.

### Sulfonation of cardanol

Cardanol (10 g, 33 mmol) was sulfonated by dissolving Cardanol in methanol (100 mL) in a 250-mL round-bottom flask and cooling in an ice bath to about 5 °C. To this solution, the oleum (10.5 g, 58.93 mmol) in a dropping funnel was added slowly over 2 h [28]. The reaction mixture was allowed to stir at 90 °C for 3 h. After the stirring was completed, the mixture was allowed to cool to room temperature, then filtered and extracted using EA and water. The EA layer was washed with water several times to get the pH nearly 7 followed by the separation using separating funnel. EA was then removed under vacuum to obtain sulfonated Cardanol (SC) (*yield*=91.8%; *CHNS analysis*; *C*=66.63, *H*=7.99, *S*=8.47; *C\**=66.31, *H\**=7.15, *S\**=7.78; \*experimental).

### Reaction of SC with ECH

In a three-necked round-bottom flask equipped with condenser sulfonated cardanol (3.54 g, 9.24 mmol) and ECH (10.26 g, 110.9 mmol) were added along with TBAB (0.29 g, 0.924 mmol) as a phase transfer catalyst and toluene as a solvent. The mixture was stirred for 2 h at 120 °C. Then, the temperature was dropped down to 60 °C and NaOH (0.36 g, 9.24 mmol) was added along with CaO (0.51 g, 9.24 mmol) and the reaction continued for 5 h. Then, the solid residue was filtered off and toluene was evaporated using rotary vacuum evaporator from the filtrate to obtain intermediate (ESC) (*yield*=88.7%; *CHNS analysis*; *C*=66.33, *H*=7.89, *S*=7.38; *C\**=66.16, *H\**=7.01, *S\**=6.74; \*experimental).

### Hydrolysis of ESC

ESC was finally hydrolyzed to impart dual functionality by introducing two –OH groups which can be utilized to incorporate the sulfonated cardanol molecule in polymer backbone of waterborne polyurethane dispersion.

A round-bottom flask equipped with a magnetic stirrer was charged with SC (2.45 g, 5.57 mmol) product of step 1 along with HCl (5 mL) and water (10 mL) and stirred at 90 °C for 1 h. The reaction mass was extracted using EA and water, and EA was removed under vacuum to form the molecule (HESC) (*yield*=87.9%; *CHNS analysis*; *C*=63.69, *H*=8.02, *S*=7.08; *C\**=63.19, *H\**=7.11, *S\**=6.29; \*experimental).

### WPUD preparation

IA-based polyol made from previously reported procedure [29] (1.02 g, 3.89 mmol) and HESC (1.11 g, 2.43 mmol) along with DBTDL catalyst (0.2% batch) and acetone

as a solvent (8 mL) were charged into the round-bottom flask under stirring in the presence of  $N_2$  gas inlet. IPDI (2.61 g, 15.02 mmol) mixed in acetone (5 mL) was added dropwise under mechanical stirring. The reaction temperature was slowly increased to reflux and maintained for the next 3 h. Then, neutralization was done by addition of TEA (0.24 g, 2.43 mmol) and stirring continued for another 3 h. The reaction was continued until the desired NCO content value using dibutylamine back-titration method, followed by the chain extension with HD for 2 h. After decreasing the temperature to 45 °C, WPUD was made by dropwise addition of water into the reaction mixture under high stirring (2500 rpm). Then, the dispersion was allowed to stir at room temperature for 3 h followed by acetone evaporation under vacuum. Figures 2 and 3 show the schematic of all the synthesis processes. The standard emulsion with DMPA as a dispersing agent was made by using the similar aforementioned process.

## Characterization

To evaluate the hydroxyl groups, present on SC, ESC and HESC, hydroxyl value was calculated according to ASTM D1957-86(2001) using the acetic anhydride-pyridine method. The hydroxyl value was calculated using Eq. 1,

$$\text{Hydroxyl value} = \frac{(B - S) \times N \times 56.1}{W} \quad (1)$$

where  $B$ —blank reading,  $S$ —sample reading,  $N$ —normality of KOH, and  $W$ —weight of the sample.

The epoxy equivalent weight (EEW) of ESC was evaluated according to the ASTM D-1652 by using Eq. (2). A known weight of ESC was completely dissolved in 25 mL of the hydrochlorinating agent by taking into a glass stopper Erlenmeyer flask. The mixture was kept at ambient temperature for about 20 min followed by titration against methanolic 0.1 N NaOH solution using Bromocresol red as an indicator. The blank titration was carried out under the same conditions

$$\text{EEW} = \frac{W_s \times 1000}{(B - S) \times N} \quad (2)$$

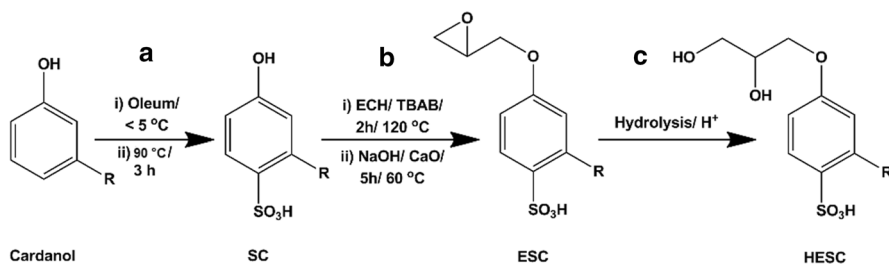


**Fig. 2** a Cardanol sulfonation; b reaction of SC with ECH; c hydrolysis of ESC

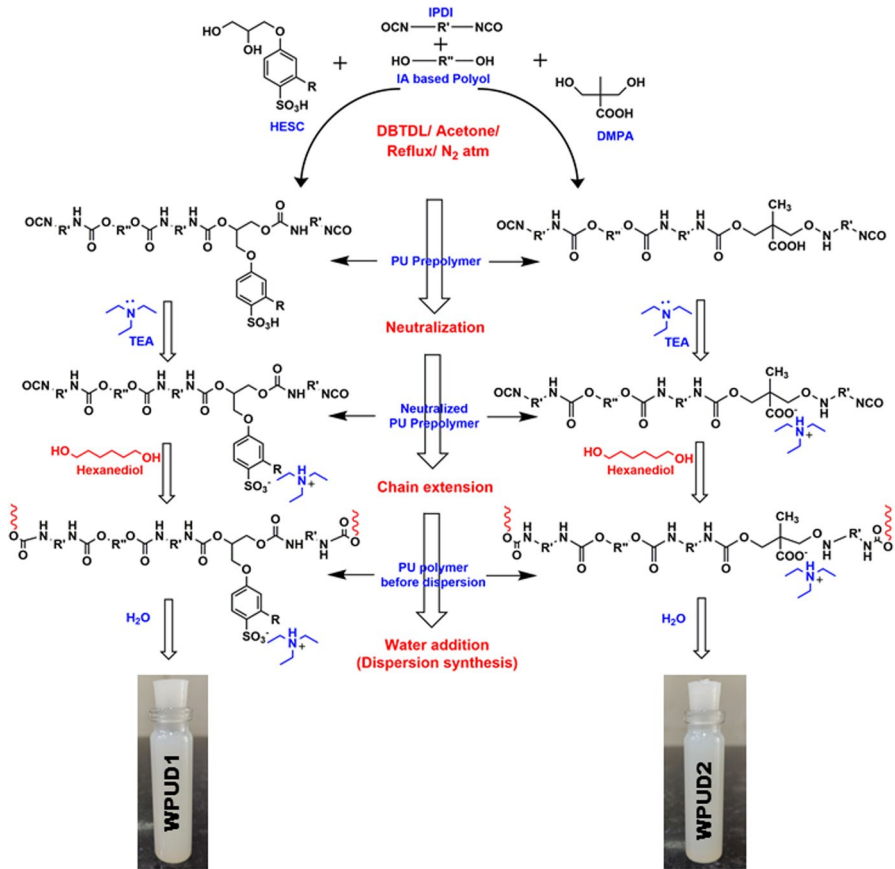


Fig. 3 Dispersion preparation process

where  $B$  is blank titration reading,  $S$  is sample titration reading,  $N$  is the normality of NaOH, and  $W_s$  is the weight of the sample in g.

To determine the gel content, the cured films were carefully peeled off from the Teflon sheet. The known weight of polymer film was kept in the solvent mixture (50:50) of xylene and dimethylformamide (DMF) at room temperature for 24 h followed by the drying of the film at 80°C until a constant weight was achieved. The gel content of the cured film was then determined by the formula;

$$\text{Gel content (\%)} = \frac{\text{Weight of the coating after 24 h of solvent immersion}}{\text{Initial weight of the coating}} \times 100 \tag{3}$$

ASTM D570 was used to determine the water absorption of the cured coating film in which the film was weighed before soaking into the water for 24 h. After 24 h, the film was removed from the water and dried with a paper towel to achieve a constant weight. Water absorption was determined from the differences

in the weight of samples before and after soaking the water according to the following equation,

$$\text{Water absorption (\%)} = \frac{(W_f - W_i)}{W_i} \times 100 \quad (4)$$

$W_f$  = final weight of the coating after water absorption test.  $W_i$  = initial weight of the coating before water absorption test.

Fourier transform infrared (FTIR) spectroscopy was carried out after loading of each polyelectrolyte layer using Bruker spectrophotometer, USA. The spectra were observed in the 600 to 4000  $\text{cm}^{-1}$  wavenumber range. The structure confirmation of HESC and intermediates was done by  $^1\text{H}$  nuclear magnetic resonance (NMR) spectroscopy. NMR spectra of the product were analyzed using Bruker DPX 800 MHz spectrophotometer with dimethyl sulfoxide (DMSO) as a solvent. The CHNS elemental analysis of compounds was done using Thermo Scientific™ FLASH™ 2000 organic elemental analyzer (OEA). The combustion of the samples was done at an elevated temperature of around 1100 °C in the presence of excess oxygen.

The particle size distribution and zeta potential measurements were taken by NanoPlus DLS particle size and zeta potential analyzer, particulate systems, Micromeritics Instrument Corporation, USA.

Thermogravimetric analysis (TGA) of cured WPUD films was conducted on PerkinElmer TGA 4000 instrument under the nitrogen atmosphere. Thermal analysis monitored in the temperature range 40–600 °C with 20 °C/min heating rate. Differential scanning calorimetry (DSC) (TA Q100 analyzer, USA) was employed for the determination of the glass transition temperature ( $T_g$ ) of cured films. The film sample weighed accurately in an aluminum pan and heated in 40 to 120 °C temperature range with a heating rate of 10 °C/min.

The coatings were characterized by performing various mechanical tests according to ASTM standards. The mild steel panels were used as the substrate for carrying out the coating characterizations on which the dispersions were applied using the spatula and allowed to dry to form films at room temperature for overnight followed by drying at 60 °C for 1 h. The adhesion of the coating to the substrate was examined by the cross-cut test according to ASTM D-3359. On the coating surface, a lattice marking of 1  $\text{cm}^2$  was done until the metal surface was exposed followed by the application of adhesion tape over lattice marking. The adhesive tape was then pulled out from the coating surface and adhesion failure was examined over the lattice marking as per ASTM standard. The pencil hardness test was carried out according to the ASTM D-3363. Scratch was made on the coating surface by using 6B to the 6H range of pencils at an angle of 45°. The impact properties of the coatings were evaluated by dropping a weighted ball of 1.36 kg from the maximum height of 60 cm onto the coated surface. The flexibility of the coatings was evaluated by using conical mandrel as per ASTM D-522. The coated panels were fixed onto a conical mandrel and were bent to analyze the coating flexibility.



**Table 1** Physicochemical analysis of SC, ESC and HESC

	Hydroxyl value (mg KOH/g resin)		EEW	
	Theoretical	Practical	Theoretical	Practical
SC	148.3	147.2	–	–
ESC	–	–	217.1	215.2
HESC	248.1	243.8	–	–

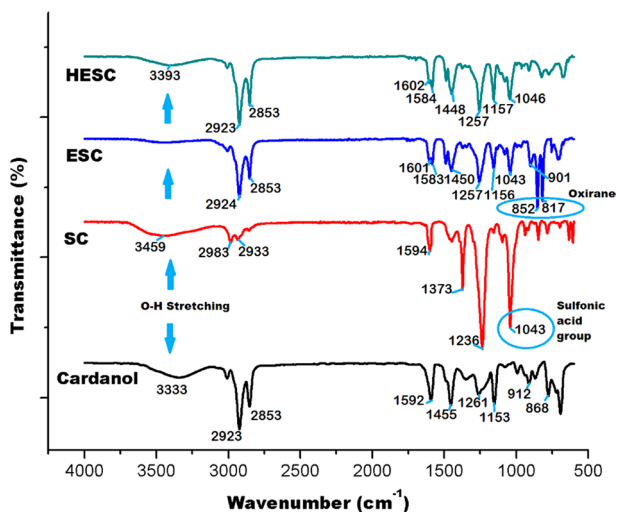


**Fig. 4** FTIR spectra of cardanol, SC, ESC and HESC

## Results and discussion

### Physicochemical analysis

All the synthesis reactions of SC, ESC and HESC were monitored by performing hydroxyl value and EEW which are then compared with theoretical values and depicted in Table 1. The results revealed that the obtained practical values are comparable with the theoretical values and the desired structures might have formed.

### FTIR and NMR analysis

Figure 4 shows the comparison between the FTIR spectra of cardanol and SC. The plateau region around 3459  $\text{cm}^{-1}$  and 3333  $\text{cm}^{-1}$  shows the presence of phenolic O–H stretch in the compound, while the peaks in the region of 2933–2983  $\text{cm}^{-1}$  show the presence of side chain aliphatic C–H stretching vibrations. The peak at 1592  $\text{cm}^{-1}$  is attributed to the C=C stretching vibration present in the aromatic ring,

and the peak around  $1447\text{ cm}^{-1}$  shows the presence of C-H deformation vibration. The peaks around  $1236\text{--}1261\text{ cm}^{-1}$  correspond to C-O stretching vibrations in phenol, while the peaks around  $847\text{ cm}^{-1}$  are attributed to the C-C skeleton vibrations. The newly formed peak at  $1043\text{ cm}^{-1}$  in the FTIR spectra of SC is the characteristic peak of the sulfonic acid group present in SC.

The confirmation of epoxidation was done by the newly formed peaks at  $852\text{ cm}^{-1}$  and  $817\text{ cm}^{-1}$  which are present in FTIR spectrum of ESC, while the increased intensity of the peak at  $3393\text{ cm}^{-1}$  and disappearance of the peaks at  $852\text{ cm}^{-1}$  and  $817\text{ cm}^{-1}$  suggest the complete hydrolysis of ESC to form HESC.

The  $^1\text{H-NMR}$  spectrum of HESC is shown in Fig. 5. The characteristic peak of the sulfonic acid proton is located at the 4.94 ppm, while the hydroxyl protons are located in the range of 0.79–0.82 ppm. The peaks around 3.35 ppm, 3.69 ppm and 3.9 ppm are associated with the protons present in ECH. The peaks at 6.7 ppm, 6.71 ppm and 7.13 ppm are attributed to the protons present in the aromatic benzene ring of cardanol, while the side chain aliphatic protons are distributed at various deviations like 4.9 ppm, 5.28–5.73 ppm, 2.4–2.5 ppm, 1.87 ppm, 1.94 ppm, 1.48 ppm, 1.22 ppm and 1.19 ppm.

## DLS spectroscopy

The particle size and zeta potential analysis was carried out using DLS spectroscopy, and the results obtained are depicted in Table 2 and particle size–intensity distribution is shown in Fig. 6. The particle size of the WPUD1 was lower than that of the WPUD2 which can be attributed to the higher dispersion capability of the sulfonic acid groups than that of the carboxylic acid groups into the water. The zeta potential values suggest that WPUD1 particles had slightly lower dispersible

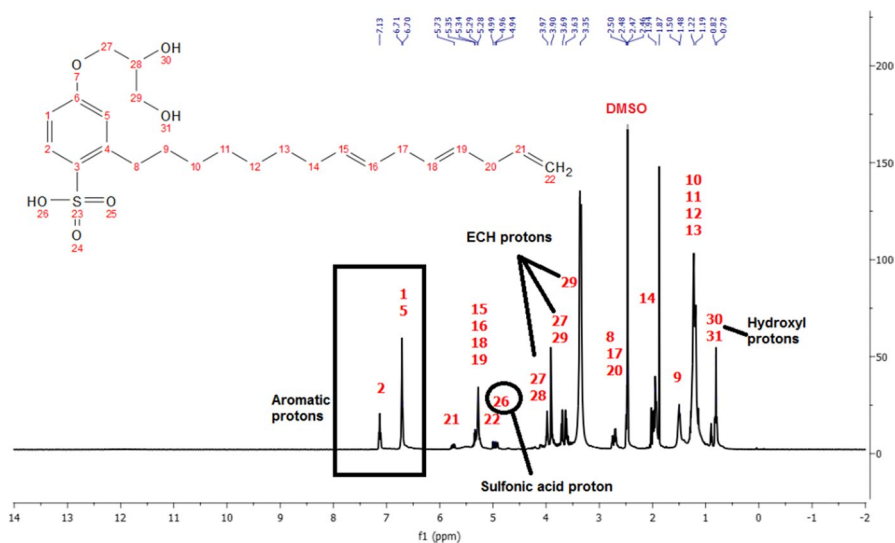
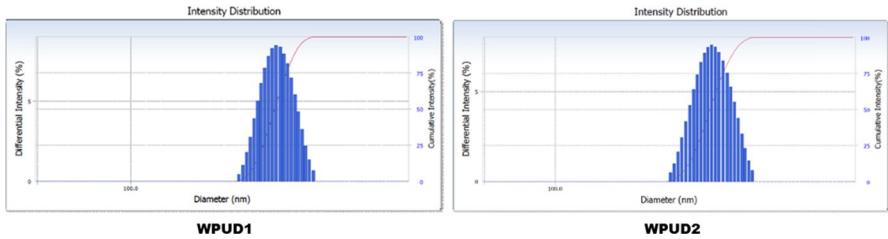


Fig. 5  $^1\text{H-NMR}$  spectrum of HESC

**Table 2** Particle size and zeta potential results of WPUDs

	Particle size (nm)	Polydispersity index (PDI)	Zeta potential (mV)
WPUD1	317.8	0.084	− 32.89
WPUD2	375.9	− 0.429	− 57.88



**Fig. 6** Particle size–intensity distribution of WPUDs

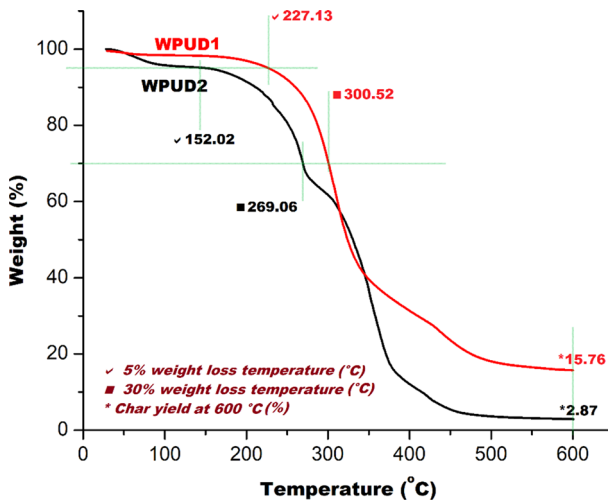


**Fig. 7** TGA curves of cured WPUD films

charges and slightly lower stability than WPUD2. WPUD2 particles were more uniformly distributed in the dispersion than that of WPUD1, and hence, its settling took a slightly longer time. [30]

**Thermal Properties**

TGA of the cured samples was done to study the changes in the physical and chemical properties of the agent. TGA and DTG curves of cured coating samples are shown in Figs. 7 and 8, respectively, while the characteristic thermal behavior

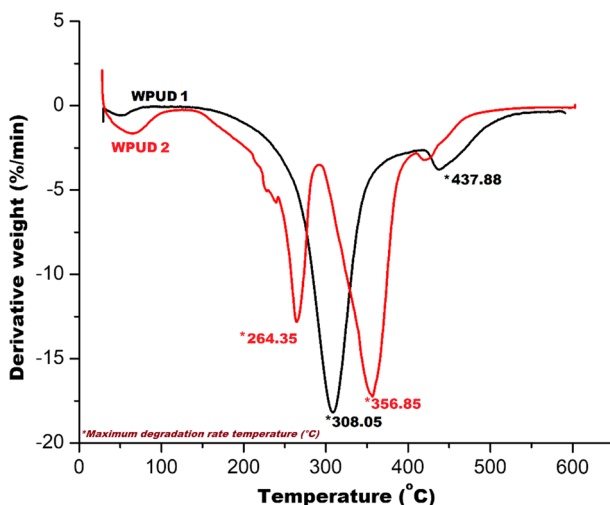


Fig. 8 DTG curves of cured WPUD films

Table 3 Thermal characteristic values of cured WPUD films

	$T_g$ (°C)	5% weight loss [T5] (°C)	30% weight loss [T30] (°C)	$T_{HRI}$ (°C)	% Residue at 600 °C
WPUD1	78.0	227.1	300.5	132.8	15.7
WPUD2	68.7	152.0	269.0	108.8	2.8

of the cured samples is depicted in Table 3. The initial degradation temperatures of the polymeric matrices are dependent on the volatile matter and the initial chain relaxations due to the thermal energy. Along with the incorporation of thermally stable sulfur (S) atoms, the bulky nature of the HESC is supporting the overall thermal stability of the coating film. The initial degradation of the polymeric network in WPUD1 has increased than that of WPUD2 which can be attributed to the higher amount of energy required for the chain relaxation and to the competency of the bulky nature of HESC and simultaneous incorporation of the thermally stable S atoms. Furthermore, the later stage of degradation also showed a significant increase in the thermal stability of the coating film of WPUD1. TGA of WPUD1 shows 5% and 30% weight loss temperature at 227.1 °C and 300.5 °C, while WPUD2 shows at 152 °C and 269 °C, respectively. The initial thermal degradation temperature of polyurethane is dependent also on the degradation of soft segments and chain packing density. The hard segments are periodically or may be randomly placed in the polymeric backbone which decides the stacking of the polymer chains over one another. In the case of WPUD1, the dispersing agent (HESC) had the bulky structure which might have restricted the chain mobility and degradation of soft segments at the initial stage. The latter stage of degradation as said earlier depends upon the degradation of the hard segments, i.e., aromatic-rigid rings, stiff sites like urethane linkages and inherent stability of

sulfur atoms which are harmoniously supporting the thermal resistance at higher temperatures. Furthermore, the residue obtained, i.e., char yield of the products at 600 °C, showed a drastic difference between the values where WPUD1 had 15.7% char yield, whereas WPUD2 had only 2.8%. Although the thermal stability of the sulfonic acid-containing polymers is less than that of the other thermally stable polymeric-variants, the stability observed in WPUD1 is higher than that of the other WPUDs synthesized from carboxylic acid-dispersing agents.

The DTG curves denote the temperature at which the degradation rate was maximum. The temperature for the maximum degradation rate at the first stage of degradation showed the significant hike for WPUD1 of about greater than 40 °C which suggests the successful incorporation of S atoms into the polymeric matrix [7, 31]. DTG curves show the two-stage degradation and the temperature of maximum degradation rate. WPUD2 indicates first maximum degradation rate at 264.35 °C, while WPUD1 had the same stage at a higher temperature – 308.05 °C. Moreover, second maximum degradation rate of WPUD2 occurred at 365.85, while that of WPUD1 at 437.88 °C which demonstrates the overall good thermal stability of WPUD1 over WPUD2. The thermal heat resistance index ( $T_{HRI}$ ) was then calculated for better perception on the thermal stability of the polymers which further elucidates that the WPUD1 had better thermal stability at elevated temperatures than that of the WPUD2 [31, 32].

$$T_{HRI} = 0.49 \times [T5 + 0.6 \times (T30 - T5)]$$

The glass transition temperature ( $T_g$ ) values of the cured WPUD samples are given in Table 3, and DSC curves are shown in Fig. 9. WPUD1 had the  $T_g$  of 78.09 °C, while WPUD2 had 68.73 °C. The results indicate that the  $T_g$  values of the cured samples increase with the incorporation of HESC into the polymer matrix. This also can be related to the presence of the phenylene ring present in the cardanol due to which the motion of the molecules is hindered which resulted in the formation of high  $T_g$  [33, 34].

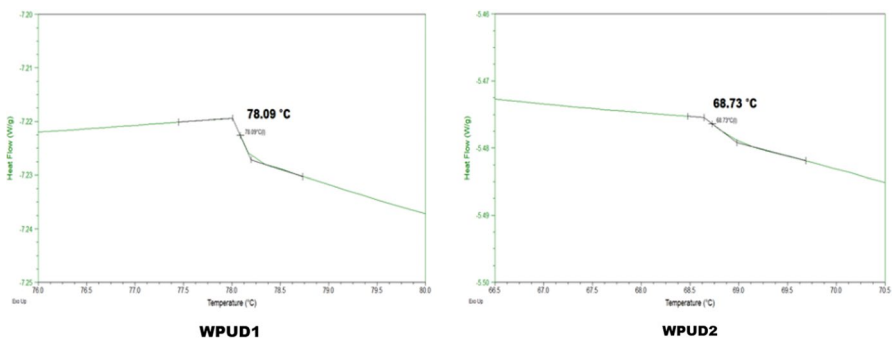


Fig. 9 DSC thermograms of cured WPUD films

## Mechanical properties

The various mechanical properties of the coatings, such as pencil hardness, flexibility, cross-cut test, were performed to determine the ability of the coating to resist mechanical stress. The results showed that the properties of the WPUD coatings varied with the incorporation of HESC in the coating system. The pencil hardness has been decreased along with the failure in flexibility which can be attributed to the bulky structure of HESC and incorporation of the benzene ring and S atoms which led to brittle film formation. The impact resistance was also lower in the case of WPUD1 than WPUD2. The cross-cut adhesion tape test also reflected similar results.

The gel content of the cured samples was evaluated in the solvent mixture of xylene and DMF for 24 h. The gel content values reflected how the nature of HESC affected the barrier properties and cross-linking density within the polymer matrix. This can be explained as the incorporation of the bulky structure is there in the polymeric system, there are increased voids between two polymeric chains which restrict the chain packing or stacking over one another.

The cured samples were immersed in water for 24 h to determine the percentage of water migrated in cured coatings. This property is governed by the cross-linking density of the material, i.e., the higher the cross-linking density, the lower the water absorption.

The solvent scrub resistance test was carried out by rubbing the samples for over 450 cycles by using MEK and xylene. The results revealed that both the cured samples are sufficiently cross-linked which prevented any defects like the dissolution of film or loss of gloss. The high resistance to solvent scrub is due to the highly cross-linked structure of the cured films and the presence of N–H or O–H groups which create a hydrogen bonding in it or with other molecules or substrate suggesting the good adhesion. The detailed results of all the tests are depicted in Table 4.

## Conclusion

Cardanol was sulfonated successfully followed by the epoxidation at phenolic hydroxyl and further hydrolysis to obtain HESC. The obtained products were thoroughly characterized by on-time reaction monitoring and analysis using the

**Table 4** Mechanical properties of cured WPUD films

	Impact test (cm)	Flexibility	Solvent scrub test (rubs)	Pencil hardness	Cross-cut test	Gel content (%)	Water absorption (%)
WPUD1	45	Fail	>250	H	Fail	81.2	2.9
WPUD2	55	Passed with little cracking		3H	Pass	89	1.4

determination of hydroxyl value, epoxy equivalent weight, CHNS analysis, FTIR analysis and the confirmation of the structure of the final product using  $^1\text{H-NMR}$ . The obtained sulfonated reactive dispersing agent was then successfully incorporated into the polyurethane backbone to obtain WPUD. The particle size determination and zeta potential analysis were performed for the characterization of obtained WPUDs. The properties were always compared with the standard dispersion obtained using DMPA as a dispersing agent, while thermal properties of the coating films revealed that the initial and final degradation temperatures were significantly increased along with the temperature of maximum degradation rate. The better inherent thermal stability of WPUD1 was attributed to the incorporation of the benzene ring and S atoms in the PU backbone. The mechanical properties did not show improvement which was the result of poor chain stacking because of the bulky nature of the obtained HESC. The obtained sulfonated difunctional dispersing agent can be incorporated into the other formulations with different polyols or diisocyanates along with the change in a polymeric backbone such as epoxy to obtain desired properties as per the end application.

## References

1. Chattopadhyay DK, Raju KVS (2007) Structural engineering of polyurethane coatings for high performance applications. *Prog Polym Sci* 32:352–418. <https://doi.org/10.1016/j.progpolymsci.2006.05.003>
2. Nečasová B, Liška P, Kelar J, Šlahof J (2019) Comparison of adhesive properties of polyurethane adhesive system and wood-plastic composites with different polymers after mechanical, chemical and physical surface treatment. *Polymers (Basel)* 11:15–17. <https://doi.org/10.3390/polym11030397>
3. Segura DM, Nurse AD, McCourt A et al (2005) Chemistry of polyurethane adhesives and sealants. *Handb Adhes Sealants* 1:101–162. [https://doi.org/10.1016/S1874-5695\(02\)80004-5](https://doi.org/10.1016/S1874-5695(02)80004-5)
4. Akindoyo JO, Beg MDH, Ghazali S et al (2016) Polyurethane types, synthesis and applications—a review. *RSC Adv* 6:114453–114482. <https://doi.org/10.1039/c6ra14525f>
5. Paik Sung CS, Schneider NS (1978) Structure-property relationships of polyurethanes based on toluene di-isocyanate. *J Mater Sci* 13:1689–1699. <https://doi.org/10.1007/BF00548732>
6. Berezkin Y, Urlick M (2013) Modern polyurethanes: Overview of structure property relationship. *ACS Symp Ser* 1148:65–81. <https://doi.org/10.1021/bk-2013-1148.ch004>
7. Honarkar H (2018) Waterborne polyurethanes: a review. *J Dispers Sci Technol* 39:507–516. <https://doi.org/10.1080/01932691.2017.1327818>
8. Overbeek GC, Steenwinkel P, Tennebroek R, Nabuurs T (2003) US Patent 20030055171A1
9. Costa G, Kroutilova IA, Mercatali S, Bassi GL (2013) EP Patent 2321361B1
10. Duan Y, Dochniak MJ, Stammler S (1994) WO Patent 1995008583A1
11. Wei X, Yu X (1997) Synthesis and properties of sulfonated polyurethane ionomers with anions in the polyether soft segments. *J Polym Sci Part B Polym Phys* 35:225–232. [https://doi.org/10.1002/\(SICI\)1099-0488\(19970130\)35:2%3c225::AID-POLB3%3e3.0.CO;2-R](https://doi.org/10.1002/(SICI)1099-0488(19970130)35:2%3c225::AID-POLB3%3e3.0.CO;2-R)
12. Yang Z, Zang H, Wu G (2019) Study of solvent-free sulfonated waterborne polyurethane as an advanced leather finishing material. *J Polym Res* 26:1–13. <https://doi.org/10.1007/s10965-019-1884-4>
13. Feng J, Wang X, Guo P et al (2018) Mechanical properties and wear resistance of sulfonated graphene/waterborne polyurethane composites prepared by in situ method. *Polymers (Basel)* 10:1–12. <https://doi.org/10.3390/polym10010075>
14. Deka R, Bora MM, Upadhyaya M, Kakati DK (2015) Conductive composites from polyaniline and polyurethane sulphonate anionomer. *J Appl Polym Sci* 132:1–9. <https://doi.org/10.1002/app.41600>
15. Bottino A, Capannelli G, Comite A, Costa C (2011) Synthesis and characterization of polyurethanic proton exchange membranes. *J Fuel Cell Sci Technol* 8:2–8. <https://doi.org/10.1115/1.4003981>

16. Mannari VM (2015) US Patent 8,952,093
17. Fu C, Zheng Z, Yang Z et al (2014) A fully bio-based waterborne polyurethane dispersion from vegetable oils: From synthesis of precursors by thiol-ene reaction to study of final material. *Prog Org Coatings* 77:53–60. <https://doi.org/10.1016/j.porgcoat.2013.08.002>
18. Liang H, Feng Y, Lu J et al (2018) Bio-based cationic waterborne polyurethanes dispersions prepared from different vegetable oils. *Ind Crops Prod* 122:448–455. <https://doi.org/10.1016/j.indcrop.2018.06.006>
19. Panda SS, Panda BP, Nayak SK, Mohanty S (2018) A review on waterborne thermosetting polyurethane coatings based on castor oil: synthesis, characterization, and application. *Polym - Plast Technol Eng* 57:500–522. <https://doi.org/10.1080/03602559.2016.1275681>
20. Gedam PH, Sampathkumaran PS (1986) Cashew nut shell liquid: extraction, chemistry and applications. *Prog Org Coat* 14:115–157. [https://doi.org/10.1016/0033-0655\(86\)80009-7](https://doi.org/10.1016/0033-0655(86)80009-7)
21. Kumar PP, Paramashivappa R, Vithayathil PJ, Rao PVS, Rao AS (2002) Process for Isolation of Cardanol from Technical Cashew (*Anacardium occidentale* L. ) Nut Shell Liquid. *J Agric Food Chem* 50(16):4705–4708. <https://doi.org/10.1021/jf020224w>
22. Shi Y, Kamer PCJ, Cole-Hamilton DJ (2019) Synthesis of pharmaceutical drugs from cardanol derived from cashew nut shell liquid. *Green Chem* 21:1043–1053. <https://doi.org/10.1039/c8gc03823f>
23. Chen J, Liu Z, Jiang J et al (2015) A novel biobased plasticizer of epoxidized cardanol glycidyl ether: synthesis and application in soft poly(vinyl chloride) films. *RSC Adv* 5:56171–56180. <https://doi.org/10.1039/c5ra07096a>
24. Balachandran VS, Jadhav SR, Vemula PK, John G (2013) Recent advances in cardanol chemistry in a nutshell: from a nut to nanomaterials. *Chem Soc Rev* 42:427–438. <https://doi.org/10.1039/c2cs35344j>
25. Mele G, Vasapollo G (2008) Fine chemicals and new hybrid materials from cardanol. *Mini Rev Org Chem* 5:243–253. <https://doi.org/10.2174/157019308785161611>
26. Lubi MC, Thachil ET (2000) Cashew nut shell liquid (CNSL)—A versatile monomer for polymer synthesis. *Des Monomers Polym* 3:123–153. <https://doi.org/10.1163/15685500300142834>
27. Bruce IE, Mehta L, Porter MJ et al (2009) Anionic surfactants synthesised from replenishable phenolic lipids. *J Surfactants Deterg* 12:337–344. <https://doi.org/10.1007/s11743-009-1116-8>
28. Peungjitton P, Sangvanich P, Pornpakakul S et al (2009) Sodium cardanol sulfonate surfactant from cashew nut shell liquid. *J Surfactants Deterg* 12:85–89. <https://doi.org/10.1007/s11743-008-1082-6>
29. Mestry SU, Patil DM, Mhaske ST (2018) Effect of 2-aminobenzothiazole on antimicrobial activity of waterborne polyurethane dispersions (WPUDs). *Polym Bull.* <https://doi.org/10.1007/s00289-018-2469-9>
30. Dogan NA (2014) Thesis: Synthesis and Characterization of novel waterborne polyurethane dispersions. Sabanci University, Graduate School of Engineering and Natural Science
31. Honarkar H, Barmar M, Barikani M (2015a) New sulfonated waterborne polyurethane dispersions: preparation and characterization. *J Dispers Sci Technol* 2691:151006122122007. <https://doi.org/10.1080/01932691.2015.1028071>
32. Honarkar H, Barmar M, Barikani M (2015b) Synthesis, characterization and properties of waterborne polyurethanes based on two different ionic centers. *Fibers Polym* 16:718–725. <https://doi.org/10.1007/s12221-015-0718-1>
33. Anderson JT (2003) US Patent 6,649,727 B1
34. Gao R, Zhang M, Dixit N, Moore R, Long T (2012) Influence of ionic charge placement on performance of poly(ethylene glycol)-based sulfonated polyurethanes. *Polymer* 53:1203–1211. <https://doi.org/10.1016/j.polymer.2012.01.043>

**Publisher's Note** Springer Nature remains neutral with regard to jurisdictional claims in published maps and institutional affiliations.